

Mössbauer studies of ferromagnetic metallic glasses under high pressure

B. Bouzabata* and R. Ingalls

Physics Department, University of Washington, Seattle, Washington 98195

K. V. Rao

Central Research Laboratory, 3M Company, St. Paul, Minnesota 55133

(Received 15 February 1983; revised manuscript received 21 December 1983)

An investigation of the Mössbauer effect in several ferromagnetic metallic glasses at high pressure is reported. The amorphous alloys studied were of the form $(\text{Fe}_x\text{Ni}_{1-x})M$, where M is a combination of the metalloids P, B, Si, or Al, and x varies from 0.34 to 0.47. In these materials the Curie temperatures were observed to decrease with pressure at a rate varying from -0.16 to -0.50 K/kbar. Such behavior is consistent with the simpler itinerant models of ferromagnetism at low pressures, but deviates at the higher pressures, possibly due to inhomogeneities. The magnetic hyperfine spectra were analyzed by decomposing them into hyperfine field distributions, $P(H)$. The average hyperfine fields and their pressure derivatives, qualitatively, behave similar to crystalline Fe-Ni alloys. From the behavior of the pressure dependence of the width of the distributions, one is able to draw some conclusions as to the short-range—versus—long-range nature of the magnetic interactions. The volume dependence of the isomer shifts in these materials suggests an inference as to the near-neighbor coordination of the iron atoms.

I. INTRODUCTION

Recently, metallic glasses containing iron have been the object of considerable attention.¹ This interest has certainly reflected the great technological importance of these materials as well as their theoretical significance. Their unusual properties are a serious challenge to one's microscopic picture. That these materials are ferromagnetic adds yet another dimension. In fact, such systems appear to be good examples of weak itinerant ferromagnetism.² For example, magnetic studies of some amorphous alloy systems appear to exhibit Invar-like characteristics such as low thermal expansion and large volume magnetostriction.³

Although a clear picture of the chemical and structural disorder, especially the short-range order, is still lacking, Mössbauer investigations have begun to shed some light as to the influence of amorphous structure on the magnetic properties.⁴⁻⁶ Similarly, high-pressure experiments² have been shown to be important in this area. In particular, the pressure dependences of the Curie temperature and the magnetization (or hyperfine field) provide measures of fundamental quantities related to the exchange interactions, bandwidth, and its fine structure.⁷ Furthermore, the influence of the structural disorder on the local surrounding of the iron nucleus may be examined under pressure by the Mössbauer technique.

Here, we report the effects of high pressure on the Curie temperatures T_C , hyperfine fields H , and velocity shifts S in several metallic glasses. Quadrupole splittings and their distribution are reported for atmospheric pressure.

The four metallic glasses studied were chosen for their relative Curie temperature T_C and their relative iron to nickel concentration, as well as their metalloid content.

Here, we summarize the composition of these materials. They are classified according to iron concentration, metalloid concentration M , and by $x = [\text{Fe}]/[\text{Fe} + \text{Ni}]$:

Alloy no.		x	M
32	$\text{Fe}_{32}\text{Ni}_{36}\text{Cr}_{14}\text{P}_{12}\text{B}_6$	0.47	0.18
30	$\text{Fe}_{30}\text{Ni}_{45}\text{P}_{16}\text{B}_6\text{Al}_3$	0.40	0.25
29	$\text{Fe}_{29}\text{Ni}_{49}\text{P}_{14}\text{B}_6\text{Si}_2$	0.37	0.22
27	$\text{Fe}_{27}\text{Ni}_{53}\text{P}_{14}\text{B}_6$	0.34	0.20

II. EXPERIMENTAL AND DATA ANALYSIS CONSIDERATIONS

Mössbauer data were taken for absorbers of alloys 30, 29, and 27 at different temperatures (up to 440 K) and pressures up to 100 kbar. For alloy 32, the low-temperature data were previously taken by Liu *et al.*⁸ in a different experimental system.⁹ Here that data have been given further analysis. The Mössbauer source was 25 mC of ^{57}Co in Rh at room temperature.

A. Pressure cell

High pressures were generated in a pressure cell discussed previously.¹⁰ A gasket 0.5 mm thick with a central hole 0.8 mm in diameter containing the sample, plus epoxy was sandwiched between two Bridgman-type anvils, with a boron-carbide tip 2.5 mm in diameter flat. Typical samples of alloys 30, 29, and 27, roughly circular and etched to a thickness of about 25 μm , were subjected to pressures up to 100 kbar. Pressure calibration was done with the use of the ruby fluorescence technique.¹¹ The

two fluorescence lines, $R1=6942 \text{ \AA}$ and $R2=6928 \text{ \AA}$, emitted by a ruby chip, shift linearly with pressures. The ruby chip is placed in the hole of a gasket and squeezed between two anvils of identical flat size, one of which has a transparent diamond tip, in order to optically excite, via a laser, the ruby crystal under pressure. The shift of the fluorescence lines is recorded, giving a pressure reading. The quite reproducible, sample-pressure-versus-applied-force relationship obtained above, for a given gasket type, was used for the actual Mössbauer experiment. The accuracy of this pressure calibration is estimated to be better than 5%, up to 70 kbar. Between 70 and 100 kbar, the accuracy reduces to perhaps 10% at the highest pressures.

B. Curie temperature

The Curie temperatures T_C were determined by the thermal scanning method.¹² In such a method, the sample temperature is varied as the source-absorber relative velocity is kept constant, usually at zero velocity. An abrupt increase in the transmitted γ -ray counting rate, or decrease in the Mössbauer absorption, is observed when the system changes from the paramagnetic to the ferromagnetic state due to the onset of the magnetic order (Fig. 1). For alloys 27 and 29, one sample is used for only one temperature scan at a given pressure to avoid annealing effects which are known to raise T_C .^{13,14} For alloy 30, the same sample was used for all runs, with no changes of T_C observed. The temperature was controlled to better than 0.5 K.

C. Hyperfine fields

The broad Mössbauer spectra due to the range of structurally and magnetically inequivalent sites of iron present in an amorphous metallic glass^{15,16} are well characterized by a distribution of hyperfine fields $P(H)$ defined by its peak value H_{peak} , its maximum value H_{max} , its half width at half height ΔH , and its average value or effective value

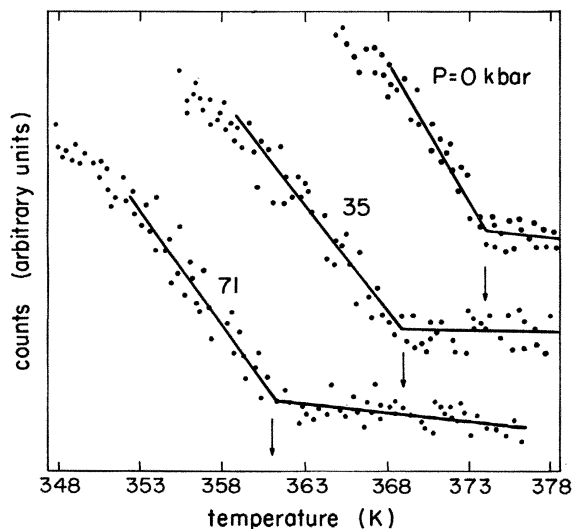


FIG. 1. Thermal scan results at several pressures for alloy 27.

$$H_{\text{eff}} = \frac{\int P(H)H dH}{\int P(H)dH}$$

This type of analysis follows a method due to Window,¹⁷ and includes optimizing an additional parameter, b , the intensity of the second or fifth line of the six Mössbauer lines.¹⁵ The parameter b depends on the angle θ between the magnetization direction and the γ rays. For the 14.4-keV state of ^{57}Fe , the six-line pattern has an expected intensity ratio for $3:b:1:1:b:3$, where $b = 4 \sin^2\theta / (1 + \cos^2\theta)$ varies from 0 (all moments are parallel to the γ -ray direction) to 4 (all moments are perpendicular to the γ -ray direction). Polarization methods, using a small laboratory magnet, were used to check the qualitative consistency of the b values obtained from the fit. In general, reasonably good fits were obtained for a constant linewidth $W=0.30$ mm/s. The electric quadrupole splitting below T_C was neglected due to the averaging over angular variations¹⁸ between magnetization direction and quadrupolar axes.

III. RESULTS

A. Pressure dependence of the Curie temperature

The dependence of T_C upon pressure is shown in Fig. 2, where we have included the previous results for alloy 32.⁸ In general, T_C decreases linearly with pressure up to 40 kbar. At low pressures, this decrease is well described by the weak-itinerant-electron model¹⁹ of ferromagnetism, where it is found that

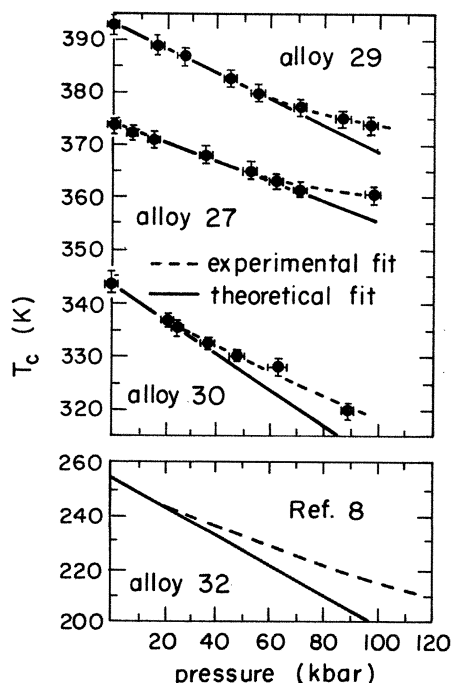


FIG. 2. Pressure dependence of the Curie temperatures of the alloys studied in this work. The solid line is predicted from simple itinerant theory.

$$\frac{dT_C}{dP} = -\frac{B}{T_C}$$

or

$$T_C(P) = T_C(0) \left(1 - \frac{P}{P_0}\right)^{1/2} \quad \text{with } P_0 = \frac{T_C^2(0)}{2B}.$$

Fits to the experimental data were carried out using the above expression for $T_C(P)$. Good fits are seen up to 40 kbar for alloys 30 and 32 and up to 70 kbar for the other alloys. The factor B above, which depends in a complex way¹⁹ upon single-particle interactions, bandwidth, and density of states, as well as many-body correlation effects, is here in the range 60–127 K²/kbar. Comparatively, this factor for the crystalline Fe-Ni alloys is much larger, being of the order of 2000 K²/kbar.²⁰ At higher pressures ($P > 40$ kbar for alloys 30 and 32 and $P > 70$ kbar for alloys 29 and 27), we note that the decrease of T_C is not as rapid as the itinerant model predicts. This might suggest that B varies (or decreases) under volume change due to changes in the bandwidth and exchange interaction. The smaller decrease in T_C can also be explained by assuming that the magnetization is not homogeneous due to spatial fluctuations of the concentration in the amorphous alloys. In that case, Wohlfarth²¹ has shown from simple assumptions and the use of the Landau-Ginzburg model,²² that the T_C dependence is written

$$\frac{dT_C}{dP} = -AT_C \quad \text{or } T_C(P) = T_C(0)e^{-AP}.$$

The parameter A in our four alloys is of order 10^{-3} kbar⁻¹. However, the Landau-Ginzburg model is still not satisfactory, at least for the amorphous alloys where T_C for the heterogeneous system (assumed amorphous) is found to increase relative to the homogeneous ones (assumed pure crystalline),²² in contrast to observations.²³

At low pressures, the change of T_C , dT_C/dP , and $d \ln T_C/dP$ is concentration dependent, being larger (in absolute value) for the lower percentages of Ni, although it has been shown that Ni itself is probably nonmagnetic in metallic glasses.^{24,25} Even though most properties of the amorphous alloys (Fe-Ni) M have a monotonic dependence on metalloid concentration, the changes of T_C with pressure is apparently not influenced by the size and/or charge-transfer effect of the metalloid. The larger change of T_C for $M=0.25$ can be explained by the relative decrease in the Ni percentage.

We have used the volume magnetostriction ($d\omega/dH$) of amorphous Fe- M alloys of high T_C , reported in Ref. 3, and amorphous Fe₇₈B₁₄Si₈,²⁶ with data from Ref. 27, to estimate dT_C/dP from the expression²⁸

$$\frac{d\omega}{dH} = \frac{T}{T_C} \frac{dM_s}{dT} \frac{dT_C}{dP} \left[1 + \alpha\beta T \frac{d \ln T_C}{dP} \right]^{-1}$$

$$\approx \frac{T}{T_C} \frac{dM_s}{dT} \frac{dT_C}{dP},$$

where M_s is the saturation magnetization. Here, α and β are the thermal expansion coefficient and the bulk

modulus, respectively. The results are shown in Fig. 3 and Table I and are compared with amorphous Fe-Ni (Ref. 29) and crystalline Fe-Ni.^{20,30,31}

Comparison of the results of both phases (crystalline and amorphous) shows similarities when dT_C/dP is plotted versus T_C . The change of T_C with pressure follows the same typical behavior in both phases. However, Invar behavior exists in the amorphous alloys with high iron content (when $x > 0.80$), in contrast to the crystalline case ($0.55 < x < 0.71$). There is no positive value of dT_C/dP in the amorphous phase with high nickel content as in the crystalline Fe-Ni alloys. In the Invar region of amorphous Fe-Ni alloys, the pressure shift of T_C is proportional to $-B/T_C$, with $B=2640$ K²/kbar (solid circles in Fig. 3). Recent measurements³² in amorphous Fe₉₀Zr₁₀, where dT_C/dP is as large as -3.8 K/kbar, have confirmed the Invar behavior in amorphous Fe- M with high iron content.

B. Hyperfine fields versus pressure

Representative Mössbauer data are shown in Fig. 4 (also see Ref. 8). Hyperfine-field distribution data obtained for the present alloys is shown in Fig. 5. At atmospheric pressure, this distribution $P(H)$ is symmetric for alloys 29 and 27, but asymmetric for the other alloys, 30 and 32. The distribution of $P(H)$ of alloy 32 is bimodal and extends to very low fields, in accordance with previous results.³³ Consequently, the half-width is unusually large [$\Delta H(P=0)=110$ kOe].

Under pressure, the general behavior is a shift of $P(H)$ to lower fields. That is, the width of the whole Mössbauer spectrum decreases, implying that H_{eff} decreases. For example, for alloy 30, the half-width of the whole spectrum is reduced by 24% for an applied pressure of 68 kbar.

For alloys 32, 29, and 27, we find the second line intensity (parameter b), which is fitted, to be roughly constant under pressure, implying that the magnetization direction does not change, although one expects anisotropic stresses. For alloy 30, the parameter b fluctuates around 1.8, increasing, on the average, at higher pressures. The reason for this is possibly due to the presence of competing ex-

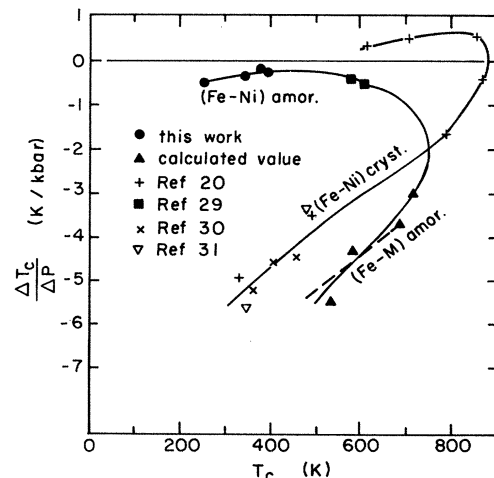


FIG. 3. Correlation between $\Delta T_C/\Delta p$ and T_C from the present work and several related systems.

TABLE I. Curie temperature T_C and its pressure dependence.

Sample	Composition	$T_C(P=0)$ (K)	$\frac{dT_C}{dP}$ (K/kbar)	$\frac{d \ln T_C}{dP}$ (kbar $^{-1}$)	Reference
Alloy 32	Fe ₃₂ Ni ₃₆ Cr ₁₄ P ₁₂ B ₆	254	-0.50	-2×10^{-3}	8
Alloy 29	Fe ₂₉ Ni ₄₉ P ₁₄ B ₆ Si ₂	393	-0.23	-5.8×10^{-4}	This work
Alloy 30	Fe ₃₀ Ni ₄₅ P ₁₆ B ₆ Al ₃	344	-0.32	-9.3×10^{-4}	This work
Alloy 27	Fe ₂₇ Ni ₅₃ P ₁₄ B ₆	373	-0.16	-4.3×10^{-4}	This work
Crystalline	Fe ₃₆ Ni ₆₄	873	-0.40	-4.5×10^{-4}	20
Amorphous alloy	$\frac{dw^a}{dH}$ (Oe $^{-1}$)	$T_C(P=0)$ (K)	$\frac{dT_C}{dP}$ (K/kbar)	$\frac{d \ln T_C}{dP}$ (kbar $^{-1}$)	Reference
Fe ₈₆ B ₁₄	60×10^{-10} (Ref. 3)	533	-5.5	-10.5×10^{-3}	Calculated
Fe ₈₄ B ₁₆	45×10^{-10} (Ref. 3)	585	-4.3	-7.5×10^{-3}	Calculated
Fe ₈₀ B ₂₀	25×10^{-10} (Ref. 3)	685	-3.7	-5.5×10^{-3}	Calculated
Fe ₇₈ B ₁₄ Si ₈	24×10^{-10} (Ref. 26)	720	-2.8	-4.0×10^{-3}	Calculated

^aForced volume magnetostriction at room temperature.

change interactions between spins.³⁴ Once an average value of b was determined, it was then held constant for each alloy so that the effects of pressure could be observed more clearly.

From the $P(H)$ at different pressures, we then summarize our observations concerning $H_{\text{eff}}(P)$ (effective field), $H_{\text{max}}(P)$, $H_{\text{peak}}(P)$, and $\Delta H(P)$, which are defined in Sec. II C.

1. Effective field versus pressure

The effective field $H_{\text{eff}}(P)$ follows the general pattern in which it decreases rapidly at low pressures ($P < 20$ kbar), levels off at intermediate pressures between 20 and 60 kbar, and then decreases again at higher pressures (Fig. 6). This decrease at higher pressures is clearly apparent in two systems (alloys 29 and 27), where $T/T_C(P)$ is larger than 0.75. For alloy 32, it is small, $T/T_C(P)$ being of the order of 0.31. This enhanced decrease of $H_{\text{eff}}(P)$ at high pressure can be explained by its dependence on T/T_C and the disorder parameter³⁵ $\delta = \Delta H(P)/H_{\text{eff}}(P)$. $H_{\text{eff}}(T)$ can be written as $H_{\text{eff}}(T) = H_{\text{eff}}(0)f(T/T_C, \delta)$. Thus the pres-

sure dependence of $H_{\text{eff}}(T)$ is

$$\frac{d \ln H_{\text{eff}}(T)}{dP} \simeq \frac{d \ln H_{\text{eff}}(0)}{dP} + \left(\frac{T}{T_C} \right) \frac{d \ln H_{\text{eff}}(T)}{dP} \frac{dT_C}{dP} + \frac{d \ln H_{\text{eff}}(T)}{d\delta} \frac{d\delta}{dP}$$

One can thus calculate the correction due to the changes of T_C under pressure, expressed by the second term. It is of the order of 0.1×10^{-3} kbar $^{-1}$. In alloy 29 this effect accounts for about 10% of the decrease of H_{eff} at $P=75$ kbar. The changes of δ also enhance this decrease at high pressures.

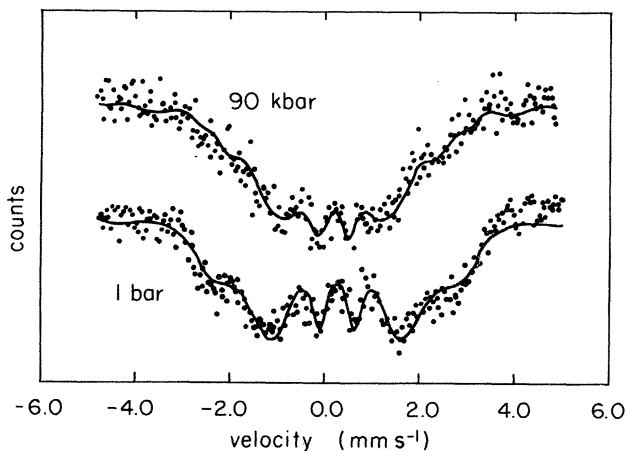


FIG. 4. Mössbauer spectra of alloy 29.

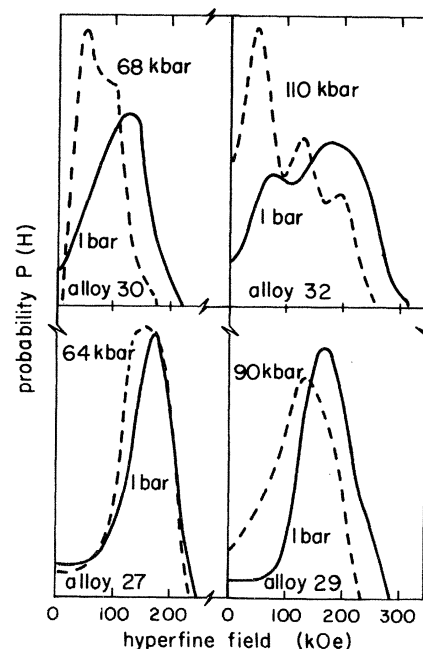


FIG. 5. Hyperfine-field distribution at low and high pressure for each of the alloys studied.

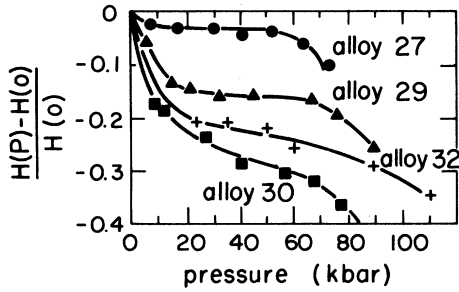


FIG. 6. Pressure dependence of the reduced effective hyperfine field for the alloys studied.

At low pressures one can neglect changes of $\delta(P)$, and the above equation reduces to

$$\frac{d \ln H_{\text{eff}}(T)}{dP} \approx \frac{d \ln H_{\text{eff}}(0)}{dP} + \left[-\frac{T}{T_C} \right] \frac{d \ln H_{\text{eff}}(T)}{dP} \frac{dT_C}{dT_C},$$

which can be used to calculate $d \ln H_{\text{eff}}(0)/dP$. Results are shown in Table II. The changes of $dH_{\text{eff}}(T)/dP$ and $d \ln H_{\text{eff}}(T)/dP$ are concentration dependent. The deviation observed for alloy 32 is clearly explained by the above discussion, and changes of hyperfine fields should be compared for similar values of $T/T_C(P)$. However, $d \ln H_{\text{eff}}(0)/dP$ vs x shows the same deviation from the linear dependence on x (for alloy 32), caused by the chromium which, as seen earlier,⁸ strongly influences the distribution of hyperfine fields.

The ratio R of the logarithmic pressure derivative of $H_{\text{eff}}(T)$ to that of T_C ,

$$R = \frac{d \ln H_{\text{eff}}(T)/dP}{d \ln T_C/dP},$$

is plotted as a function of T/T_C (Fig. 7). In the itinerant-electron model,³⁶ it was shown that the ratio of

$$\sigma = \frac{d \ln M(T)/dT}{d \ln T_C/dT}$$

is proportional to

$$\left[1 - \frac{T^2}{T_C^2} \right]^{-1}.$$

Since $H_{\text{eff}}(T)$ is expected to have the same temperature dependence as $M(T)$, one then expects that R behaves as σ . However, as seen in Fig. 7, R deviates from σ , varying somewhat as $A(T/T_C) + B$. This large deviation may be due to inhomogeneities (the constants A and B) not introduced in the above derivation, where a special shape of

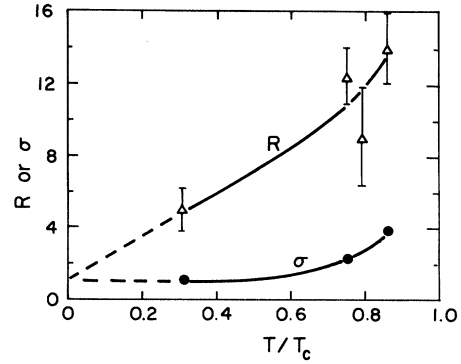


FIG. 7. Comparison of the logarithmic pressure derivative ratio $R = (d \ln H_{\text{eff}}/dp)/(d \ln T_C/dp)$ with the function $\sigma = [1 - (T/T_C)^2]^{-1}$.

$M(T) = M(0)f(T/T_C)$ was used. The disorder parameter δ also has to be introduced in $M(T)$ to improve agreement with the amorphous case or $M(T) = M(0)f(T/T_C, \delta)$.

2. Pressure dependence of H_{max} and H_{peak}

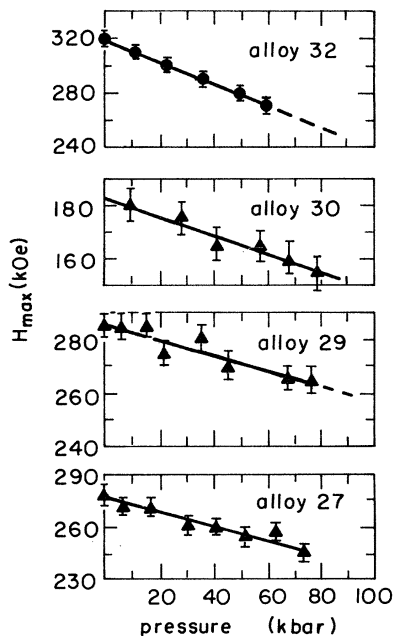
The parameter H_{max} represents the largest hyperfine field present in the amorphous alloy, while H_{peak} is the most probable field. We find that both decrease with pressure (Figs. 8 and 9). H_{max} decreases linearly for all pressure runs. Although this decrease is large, it cannot explain the even larger reduction of the whole width of the Mössbauer spectra. For example, in alloy 30 the decrease in H_{max} accounts for roughly one-half of the decrease of the width of the Mössbauer spectrum observed at an applied pressure of 68 kbar. Changes of H_{peak} might account for these differences. When the distribution $P(H)$ is not too broad, as in alloys 29 and 27, H_{peak} is well defined and decreases linearly with pressures, correlating well with dH_{max}/dP . The lower decrease of H_{peak} with pressures relative to that of H_{max} is an indication of the more asymmetric $P(H)$ observed under pressure. In alloy 32, however, both components (see Fig. 5) of the $P(H)$ distribution move to lower fields at low pressures ($P < 35$ kbar) then remain constant, while H_{max} continues to decrease linearly up to high pressures.

3. Half-width $\Delta H(P)$

In alloy 32, where Cr is present, $\Delta H(0)$ is large [$\Delta H(0) = 110$ kOe] and shows the large broadening influence of Cr atoms. However, for the other alloys $\Delta H(0)$ is close to 50 kOe, being 58, 50, and 47 kOe for alloys 30, 29, and 27, respectively. $\Delta H(0)$ varies linearly with M or

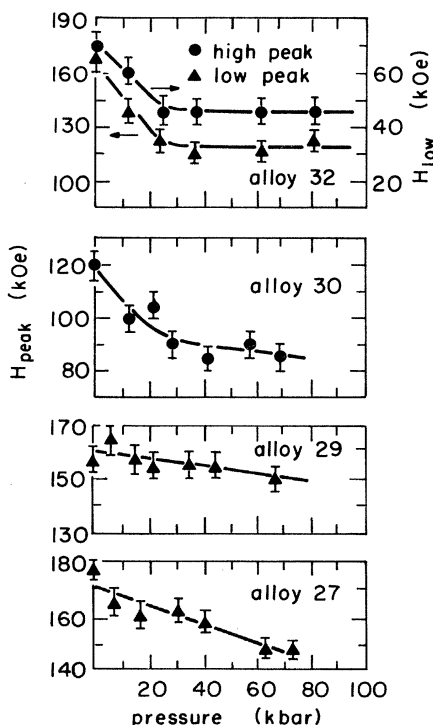
TABLE II. Results of the hyperfine-field determinations and their pressure dependence for the four amorphous alloys.

Sample	$H_{\text{eff}}(P=0)$ (kOe)	dH_{eff}/dP (kOe/kbar)	$\frac{d \ln H_{\text{eff}}(T)}{dP}$ (kbar ⁻¹)	$\Delta H(P=0)$ (kOe)	$\delta(P=0)$	dH_{max}/dP (kOe/kbar)	$\frac{d \ln H_{\text{eff}}(T=0)}{dP}$ (kbar ⁻¹)	x (at. %)
Alloy 32	147	-1.50	-10×10^{-3}	112.0	0.76	-0.83	-9.88×10^{-3}	0.47
Alloy 30	103	-1.42	-13×10^{-3}	58.0	0.58	-0.35	-11×10^{-3}	0.40
Alloy 29	165	-1.22	-7.3×10^{-3}	50.0	0.30	-0.28	-6.8×10^{-3}	0.37
Alloy 27	156	-0.46	-2.9×10^{-3}	47.0	0.28	-0.29	-2.5×10^{-3}	0.34

FIG. 8. Pressure dependence of H_{\max} .

the fractional concentration of metalloids.

The apparent variation with x is probably not significant, since M is also changing. In fact, Mössbauer studies of amorphous $\text{Fe}_{40}\text{Ni}_{40}\text{M}_{20}$ and $\text{Fe}_{80}\text{M}_{20}$,³⁷ where the metalloids are not varied, have found the widths of the $P(H)$ distribution to be the same, apart from a shift to lower fields in the case of the first sample. The linear dependence of $\Delta H(0)$ on M is then a clear indication that the width of the $P(H)$ distribution is correlated with the

FIG. 9. Pressure dependence of H_{peak} .

metalloid concentration.

The pressure dependence of the width $\Delta H(P)$ is influenced by the range of the magnetic interactions. In the amorphous ferromagnets, the width of the hyperfine-field distribution reflects the great difference between low- and high-field environments. In the case of long-range correlations, each individual magnetic moment would follow the same magnetization curve (i.e., the average magnetization) as a function of temperature or pressure. The distribution of hyperfine fields or the half-width $\Delta H(P)$ should then decrease monotonically under pressure or temperature change.

In the cases where the short-range order is dominant, however, the fluctuating environment is associated with a distribution of exchange interactions, characterized by the disorder parameter $\delta = \Delta H/H_{\text{eff}}$. In that case, the smaller magnetic moments would be less correlated with the average, and therefore, decrease more rapidly than the higher moments under pressure. The half-width $\Delta H(P)$ would then be first constant (or increasing slowly), since the distribution of high fields overlaps the low fields in the $P(H)$. It would then decrease at a pressure sufficiently high to affect the high fields.

Figure 10 shows $\Delta H(P)$ vs P for alloys 27, 29, and 30. All samples depict the above importance of the short-range interaction except alloy 30, where the monotonic decrease of $\Delta H(P)$ expresses perhaps a longer-range interaction behavior. This is consistent with results of $\text{Fe}_{30}\text{Ni}_{45}(\text{Pb,Al})_{25}$,³⁸ where the range of the Fe-Fe interaction was estimated to be very large due to the presence of strongly coupled spins.^{34,39}

4. Ratio $\delta = \Delta H(P)/H_{\text{eff}}$ versus pressure

Although $\Delta H(P)/H_{\text{eff}}$ is a measure of the disorder in amorphous systems, it is not necessarily equal to $\Delta J/\langle J \rangle$,⁴⁰ where ΔJ and $\langle J \rangle$ are the distribution and average value of the exchange interaction. Metalloids are not merely glass formers; they can undergo specific bonding with certain transition-metal atoms, and they influence both the hyperfine field at the nucleus and the Fe-Fe exchange interaction, but not necessarily in a simple manner. For example, it has been inferred that iron atoms couple strongly with phosphorus, but that nickel atoms

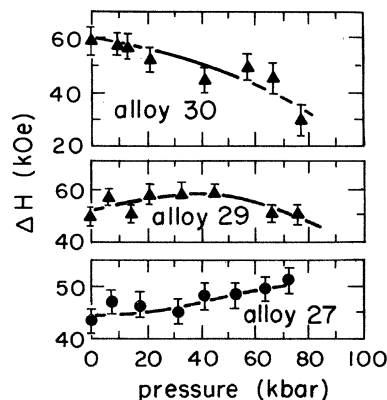


FIG. 10. Pressure dependence of the width of the hyperfine-field distributions.

have a stronger interaction with boron.⁴¹

Here, however, the percent of boron is constant in all samples. The phosphorus content varies from 12 to 16 at. %, which should equally affect the distribution of fields and the distribution of interactions.

At atmospheric pressure, δ is measured to be 0.30 for alloy 29 and 0.28 for alloy 27. In the other samples, δ is larger and might be overestimated since it is evaluated either nearer T_C or at low temperature.

We find that the parameter δ is not constant under pressures, but increases for alloys 29 and 27 (Fig. 11) and is relatively constant for alloy 30. However, in alloy 32, δ decreases at high pressures above 70 kbar. These differences in the high-pressure behavior of $\delta(P)$ correlate with the enhanced decrease of H_{eff} at high pressures in alloys 30, 29, and 27.

C. Velocity shifts versus pressures

Because of the inequivalent sites of iron present in amorphous metallic glasses, one expects a distribution of isomer shifts. However, this distribution was found to be small³⁷ in amorphous (Fe-Ni)*M*. Therefore, here we merely discuss the average velocity shift S defined as the centroid of the Mössbauer spectra.

Under pressure, the average velocity shift in each case decreases with pressure (Fig. 12, Table III) as expected,⁴² since the s -electron density at the nucleus increases. By taking a reasonable value of the bulk modulus equal to $16 \times 10^3 \text{ kg/mm}^2$,⁴³ one can calculate the relative change of the velocity shift $dS/d \ln V$. This decrease of the velocity shift for alloys 29 and 27 is found to be considerably lower than the decrease observed in the other alloys. $dS/d \ln V > 1.5 \text{ mm/s}$ for alloys 30 and 32, whereas for alloys 29 and 27, $dS/d \ln V \lesssim 1.0 \text{ mm/s}$.

This general behavior may be related to the average number of nearest neighbors $\langle z \rangle$. In crystalline alloys, it is known⁴⁴ that metals with close-packed structure (fcc or

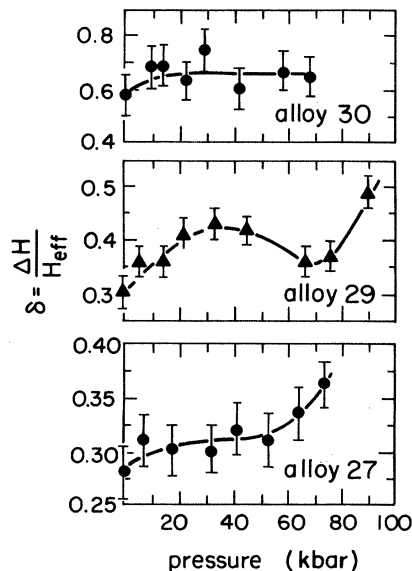


FIG. 11. Pressure dependence of the reduced width of the hyperfine distribution.

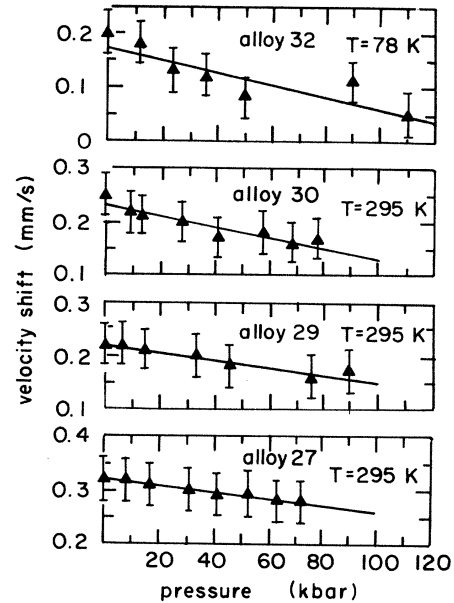


FIG. 12. Pressure dependence of the isomer shifts.

hcp) have a lower decrease of isomer shift with pressure ($dS/d \ln V \leq 1.0 \text{ mm s}^{-1}$) than bcc alloys ($dS/d \ln V > 1.0 \text{ mm s}^{-1}$). Therefore, a possible conclusion from our results is that $\langle z \rangle$, in the amorphous alloys with the higher iron content, is bcc-like, or $\langle z \rangle \approx 8$, and in alloys with lower iron concentration, it is fcc-like, or $\langle z \rangle \approx 12$. The relative decrease of the Curie temperature with increasing iron content is also consistent with less dense packing, or lower $\langle z \rangle$, since the exchange interaction is itself likely to be unchanged.

The interesting short-range atomic configuration in Fe-Ni metallic glasses has been examined in binary amorphous Fe-B alloys containing 12–25 at. % of boron by Mössbauer spectroscopy.⁴⁵ Amorphous alloys with boron content below 20 at. % exhibited well-developed short-range order with a bcc-like nearest-neighbor configuration, while amorphous Fe–25 at. % B showed a considerable fraction of chemical order of the crystalline Fe_3B type, for which each iron atom has 10 iron nearest neighbors.

The behavior of the isomer shift with pressure may also be associated with a small fractional change in the 4s-electron component on the iron atom, starting from a configuration equivalent to approximately $3d^7 4s$. In crystalline metals, this has led to an interpretation of the smaller volume dependence of the isomer shift in closed-packed structures, namely a possible enhancement of s to d transfer.^{42,44} In amorphous metallic glasses, metalloids are expected to transfer some electrons to the common d band of the transition metals. At atmospheric pressure, the large isomer shift indeed indicates that some s - p electrons are transferred to the d band of the iron atoms. The amount of electrons per transition metal (e/TM) transferred can be calculated using data of Mitera *et al.*,⁴⁶ showing (see Table III) that this amount is lower in alloys 27 and 29 than in alloy 30 (alloy 32 contains chromium which can strongly influence $dS/d \ln V$).⁴² The s to d

TABLE III. Results of the pressure dependence of the velocity shifts.

Sample	$S(P=0)$ (mm/s)	$\frac{dS}{dP}$ (mm/s kbar)	$\frac{dS}{d \ln V}$ (mm/s)	$\frac{dv}{d \ln V^a}$ (mm/s)	e/TM	$\langle z \rangle$
Alloy 32	0.15(± 0.03)	-11×10^{-4}	1.75	1.59	0.34	< 12
Alloy 30	0.25(± 0.04)	-9.6×10^{-4}	1.52	1.46	0.47	< 12
Alloy 29	0.22(± 0.04)	-6.7×10^{-4}	1.06	1.00	0.39	12
Alloy 27	0.32(± 0.04)	-6.0×10^{-4}	0.95	0.89	0.36	12

^aDeduced relative to isomer-shift change with volume after correction of the Doppler-shift contribution.

transfer under pressure would then be more favorable in alloys 27 and 29 than in alloy 30, since fewer e/TM have been transferred to the common d band in these two samples. It must be emphasized that such an interpretation of the different pressure dependences of the isomer shift between the alloys is not incompatible with the suggestion that the nearest-neighbor configurations vary. In fact, such a variation in structure may be responsible for the variation in electron transfer.

IV. SUMMARY

The pressure-induced reduction of the Curie temperature of amorphous Fe-Ni at low pressures may be explained by the standard model of weak ferromagnetism. At high pressures, however, deviations from this model, in its simplest form, have been observed, which may possibly be seen as due to inhomogeneities in the magnetization caused by local fluctuations of the concentration. The change of T_C with pressure, dT_C/dP and $d \ln T_C/dP$ (at low pressures), are linear with the iron concentration.

The change of $\Delta T_C/\Delta P$ with T_C in amorphous alloys follows the same typical behavior as in the crystalline Fe-Ni fcc alloys depicting the Invar behavior of amorphous Fe- M alloys. However, nickel atoms in amorphous alloys appear to have different magnetic behavior compared to the high-nickel-content crystalline alloys.

The dependence of the effective hyperfine fields upon pressure has a typical shape, as shown by $\Delta H(0)/H(0)$ vs P (Fig. 6). The enhanced decrease at high pressure is due primarily to the Curie-temperature dependence on volume changes. The ratio of the logarithmic pressure derivative of H_{eff} to that of T_C is found to vary as T_C^{-1} , in contrast to the expected theoretical ratio of $(1 - T^2/T_C^2)^{-1}$. As with T_C , the change of $H_{\text{eff}}(T)$ with pressure is concentration dependent. Linearly extrapolated to low iron concentration or low x , $\Delta T_C/\Delta P$ and $\Delta H_{\text{eff}}(T)/\Delta P$ approach zero for essentially the same value, $x \approx 0.30$. This value is

about the same as in the crystalline Fe-Ni fcc alloys for which $\Delta T_C/\Delta P=0$, namely $x=0.32$.⁴⁷ This critical concentration is then not dependent on structural arrangements.

The observed differences in the half-widths of the $P(H)$ distribution of the samples containing only iron and nickel are correlated with the presence of metalloids and their chemical short-range influences, rather than the changes of the ratio of $[\text{Fe}]/[\text{Ni}]$. Atoms associated with antiferromagnetism, such as chromium in alloy 32, have a drastic influence on the hyperfine-field distribution. This distribution is quite broad and bimodal (Fig. 5) where the distribution of small fields might be due to the clustering of chromium atoms around iron atoms.

Behavior of the half-width $\Delta H(P)$ of the $P(H)$ under pressure indicates that not only is short-range magnetic order (as in alloys 29 and 27) important, but that long-range interactions are important as well (as in alloy 30), even though amorphous alloys have no long-range structural order.

The relative decrease of the velocity shift under pressure may be related to two effects (nearest-neighbor configuration and effect of s to d transfer). The relative importance cannot be evaluated here although they are presumably both present. Nonetheless, comparison with the pressure effects on the transition metals shows that metallic glasses with high iron content appear to have a lower nearest-neighbor average number than the other amorphous alloys, which are regarded as possessing a high degree of short-range order.

ACKNOWLEDGMENTS

The authors gratefully acknowledge the following for help with various portions of this work: C. M. Liu, H. S. Chen, T. Egami, B. D. Dunlap, and S. Nasu. This work was supported by the National Science Foundation under Grant No. DMR-78-24995.

*Present address: University of Annaba, El-Hadjar B.B. 12, Algeria.

¹J. J. Gilman, Phys. Today **28**(5), 46 (1975); C. D. Graham and T. Egami, Ann. Rev. Mater. Sci. **8**, 423 (1978), and references therein.

²E. P. Wohlfarth, in IEEE Trans. Magn. **MAG-14**, 933 (1978).

³K. Fukamichi, H. Hiroyoshi, M. Kikuchi, and T. Masumoto, J. Magn. Mater. **10**, 294 (1974).

⁴J. Balogh, G. Faigel, M. Tegze, T. Kemeny, A. F. Schaafsma, I. Vincze, and F. Van der Woude, J. Phys. (Paris) Colloq.

C1, 255 (1980).

⁵I. Vincze, D. S. Boudreaux, and M. Tegze, Phys. Rev. B **19**, 4896 (1979).

⁶U. Gonser, M. Ghafari, and H. G. Wagner, J. Magn. Mater. **8**, 175 (1978).

⁷E. P. Wohlfarth, J. Appl. Phys. **39**, 1061 (1968).

⁸C. M. Liu, R. Ingalls, K. V. Rao, and S. M. Bhagat, J. App. Phys. **50**, 1577 (1977). See also B. Bouzabata, R. Ingalls, and K. V. Rao, J. Appl. Phys. **53**, 2324 (1982), for a preliminary report of the present results.

- ⁹C. M. Liu and R. Ingalls, *Rev. Sci. Instrum.* **49**, 1680 (1978).
- ¹⁰R. Ingalls, E. D. Crozier, J. E. Whitmore, A. J. Seary, and J. M. Tranquada, *J. Appl. Phys.* **51**, 3158 (1980).
- ¹¹G. J. Piermarini, S. Block, J. D. Barnett, and R. A. Forman, *J. Appl. Phys.* **46**, 2774 (1975); J. E. Whitmore, C. L. Bruzzone, and R. Ingalls, *Rev. Sci. Instrum.* **53**, 1063 (1982).
- ¹²R. S. Preston, S. S. Hanna, and J. Heberle, *Phys. Rev.* **128**, 2207 (1962).
- ¹³Y. N. Chen and T. Egami, *J. Appl. Phys.* **50**, 7615 (1979).
- ¹⁴H. H. Liebermann, C. D. Graham, Jr., and P. J. Flanders, *IEEE Trans. Magn.* **MAG-13**, 1541 (1977).
- ¹⁵C. L. Chien and R. Hasegawa, *Phys. Rev. B* **16**, 3024 (1977).
- ¹⁶C. L. Chien, D. Musser, F. E. Luborsky, and J. L. Walter, *J. Phys. F* **8**, 2407 (1978).
- ¹⁷B. Window, *J. Phys. E* **4**, 401 (1971).
- ¹⁸C. L. Chien, *Phys. Rev. B* **18**, 1003 (1978).
- ¹⁹D. M. Edwards and E. P. Wohlfarth, *Proc. R. Soc. London, Ser A* **303**, 127 (1968).
- ²⁰J. M. Leger, C. Loriers-Susse, and B. Vodar, *Phys. Rev. B* **6**, 4250 (1972).
- ²¹E. P. Wohlfarth, in *Physics of Solids under High Pressure*, edited by J. S. Schilling and R. N. Shelton (North-Holland, Amsterdam, 1981), p. 175.
- ²²D. Wagner and E. P. Wohlfarth, *J. Phys. F* **9**, 717 (1979).
- ²³J. Dur, *Rev. Phys. Appl.* **15**, 1036 (1980).
- ²⁴R. C. Sherwood, E. M. Gyorgy, H. S. Chen, S. D. Ferris, G. Norman, and H. J. Leamy, in *Magnetism and Magnetic Materials—1974 (San Francisco)*, Proceedings of the 20th Annual Conference on Magnetism and Magnetic Materials, edited by C. D. Graham, G. H. Lander, and J. J. Rhyne (AIP, New York, 1975), p. 745.
- ²⁵T. Mizoguchi, K. Yamauchi, and K. Miyajima, in *Amorphous Magnetism*, edited by H. D. Hooper and A. M. de Graaf (Plenum, New York, 1973).
- ²⁶T. Jagielinski, K. I. Arai, N. Tsuya, S. Ohnuma, and T. Matsumoto, *IEEE Trans. Magn.* **MAG-13**, 1553 (1977).
- ²⁷S. Hatta and T. Egami, *J. Appl. Phys.* **50**, 1589 (1979).
- ²⁸W. J. Carr, Jr., *Magnetic Properties of Metals and Alloys* (American Society for Metals, Metals Park, Ohio, 1958), p. 256.
- ²⁹J. Kamarad, Z. Arnold, J. Schneider, and S. Krupicka, *J. Magn. Mater.* **15-18**, 1409 (1980).
- ³⁰R. C. Wayne and L. C. Bartel, *Phys. Lett.* **28A**, 196 (1968).
- ³¹L. Patrick, *Phys. Rev.* **93**, 384 (1954).
- ³²K. Shirakawa, T. Kaneko, M. Nose, S. Ohnuma, H. Fujimori, and T. Masumoto, *J. Appl. Phys.* **52**, 1829 (1981).
- ³³A. S. Schaafsma, *Phys. Rev. B* **23**, 4784 (1981); C. L. Chien, *ibid.* **23**, 4788 (1981).
- ³⁴K. V. Rao, *Phys. Scr.* **25**, 742 (1982).
- ³⁵K. Hanorich, *Phys. Status Solidi B* **97**, K71 (1980).
- ³⁶B. K. Ponomarev and V. G. Thiessen, *Phys. Status Solidi B* **104**, 427 (1981).
- ³⁷I. Vincze and E. Babic, *Solid State Commun.* **27**, 1425 (1978).
- ³⁸S. M. Bhagat, M. L. Spano, and K. V. Rao, *J. Appl. Phys.* **50**, 1580 (1979).
- ³⁹S. M. Bhagat, J. A. Geohegan, and H. S. Chen, *Solid State Commun.* **36**, 1 (1980).
- ⁴⁰D. Musser and C. L. Chien, *J. Appl. Phys.* **50**, 765 (1979).
- ⁴¹R. P. Messmer, *Phys. Rev. B* **23**, 1616 (1981).
- ⁴²D. L. Williamson, in *Mössbauer Isomer Shifts*, edited by G. K. Shenoy and F. E. Wagner (North-Holland, Amsterdam, 1978).
- ⁴³C. P. Chou, *Scr. Metall.* **11**, 417 (1977).
- ⁴⁴R. Ingalls, H. G. Drickamer, and G. de Pasquali, *Phys. Rev.* **155**, 165 (1967).
- ⁴⁵R. Oshima and F. E. Fujita, *Jpn. J. Appl. Phys.* **201** (1980).
- ⁴⁶M. Mitera, N. Naka, T. Masumoto, N. Kazama, and K. Watanabe, *Phys. Status Solidi* **49**, K163 (1978).
- ⁴⁷J. S. Kouvel and R. H. Wilson, *J. Appl. Phys.* **32**, 435 (1961).